Hindawi
Complexity
Volume 2020, Article ID 2487310, 12 pages
https://doi.org/10.1155/2020/2487310

WILEY | Hindawi

Research Article

A Complex Evaluation and Optimization Approach for Oxygen-Enriched Combustion Characteristics of Blended Fuels Based on Response Surface Methodology

Y. C. Liu, H. Zhang, Z. M. Luo, S. Qing, A. M. Zhang, and S. P. Yang

State Key Laboratory of Complex Nonferrous Metal Resources Clean Utilization,
Department of Metallurgical and Energy Engineering, Kunming University of Science and Technology, Kunming 650093, China

Correspondence should be addressed to S. Qing; 15087088903@163.com

Received 16 April 2020; Accepted 8 June 2020; Published 15 July 2020

Guest Editor: Kailong Liu

With the energy consumption increasing, the coal supply in China has been becoming tight, which has made it difficult for thermal power generation in Yunnan Province. Making full use of local inferior coal and biomass resources in Yunnan can remedy the lack of fuel in power plants. In this paper, an oxygen-rich atmosphere thermogravimetric experiment was performed for a blended sample of Xiaolongtan lignite, Yiliang tobacco rod, and Fuyuan bituminous coal. The combustion characteristics of the mixed fuel under several key operating parameters (i.e., mass ratios, oxygen concentration, and heating rates) were studied. The response surface methodology was used to determine the optimal blending ratio of the three fuels. The results show that the ignition and burnout temperature of coal decrease and the combustion time diminishes with the enrichment of oxygen. The optimal oxygen concentration in the practical application is around 30%. The activation energy and preexponential factor increase with the enlargement of oxygen concentration. Such complex evaluation and optimization approach ensure the stable operation of thermal power plant production.

1. Introduction

Combustion of solid fuel plays an essential role for the social development as it provides the energy needed in the practical operation [1–3]. With the development of the electric power industry, more and more power plants have been developed by using the blended fuels combustion technology in recent years. Hence, both the academic and industrial communities have paid increasing attention to the study of blended fuels. Meanwhile, the optimization of coal blending technology can provide additional benefits such as environmental protection and effective utilization of solid fuel resources. According to the experimental observation with regard to the blended combustion, different types of coal will intensely interact [4]. The ignition temperature of blended coal varies with different amounts of blended coal at low temperatures. Increasing the proportion of high volatile coal improves the ignition, stability, and burnout characteristics of blended coal. Chen et al. [5, 6] studied the mixed combustion characteristics of two kinds of pulverized coals with different ignition characteristics and found that the ignition characteristics of the blended coal are better than those of the single coal. The ignition temperature of blended coal tends to be higher as the proportion of pulverized coal with good ignition characteristics increases. Gao et al. [7] studied the combustion characteristics of blended lignite, bituminous coal, and anthracite by thermogravimetry. It was found that when the low activation energy bituminous coal or lignite is mixed with the anthracite with high activation energy, the ignition characteristic of blended coal is the best. However, when the activation energy of two kinds of coals is similar, the activation energy of blended coal tends to be the coal with relatively high activation energy. From the combustion experiments of blended coal via the simulating combustion conditions, similar conclusions can be drawn [8–10]. The characteristics of blended coal are not a simple linear superposition of single coal. The bigger the difference of coal quality is, the more noticeable this situation will be. Peratla

et al. [11] studied the interaction of blended coal and found that the coal quality determines the combustion characteristics of blended coal, which depends on the proportion of combustible coal. Some researchers [12, 13] pointed out that the blended coal is the most critical factor in the coal combustion, and the burnout characteristics rely on the type of coal that burns slowly. At present, the studies for coal blending mainly focus on the blending of different coals while few efforts have been made to study the proportion of biomass smoke rods and coals. In addition, the performance of biomass is different from that of coal because the biomass mainly consists of high volatile substances, which have a low ignition point, rapid burning, and short burnout time. After the biomass is mixed with coal, the blended fuels have complex combustion characteristics. For the superposition of fuels, it needs to consider the coupling and synergy of the mixed fuels, which all depend on the proportion of different combustibles. In other words, the relationship between the coal blending and the main indexes of each coal composition is complexly nonlinear, which can be identified by nonlinear optimization models via response surface method (RSM) and fuzzy logic systems. Moreover, the blending ratio of blended fuels in most of the actual process is ambiguous so that the combustion performance of the blended fuels cannot be guaranteed.

Motivated by the above requirements, this article will study the optimization problem of the fuels blending via the response surface method, aiming at finding an optimal mix scheme for different fuels with the best combustion performance achieved. The flammability index, comprehensive combustion characteristic index, burnout temperature, and economic costs are chosen to characterize the advantages and disadvantages of different mixing schemes with different parameters. After validated by extensive experiments, the proposed optimization technique is utilized to find the best ratio of different fuels. The experiments are divided into 10 groups, and each group has three kinds of fuels (i.e., lignite of Xiaolongtan, tobacco rod of Yiliang, and bituminous coal of Fuyuan) with different proportions. The advantages and disadvantages of using the response surface method are analyzed, and the different proportional reference assignment schemes are discussed. The analysis and experimental results will shed light on the blending of three kinds of fuels to achieve an excellent combustion efficiency.

This paper is organized as follows: Section 2 gives the problem formulation. Section 3 gives the blended coal studies, which includes raw materials and instruments illustration, thermogravimetric analysis, and chemical structure analysis. Section 4 gives the decision analysis of the response surface method, which includes the optimization of oxygen concentration and heating rate and optimizing the proportion of blended fuel. Section 5 gives the conclusions.

2. Problem Formulation

Combustion of blended fuels should consider its ignition characteristics, volatile precipitation characteristics, slagging, burn-up, and pollutant emissions. However, the blending ratio of blended fuels in most of the actual process is blind and arbitrary so that the combustion performance of the blended fuels cannot be guaranteed. This article aims at discussing the pros and cons of different proportions of blended fuels by using the response surface method, including its flammability index, comprehensive combustion characteristics index, burnout temperature, and economic cost, and finally getting the best ratio of three kinds of fuels blended coal combustion.

Under different O_2/CO_2 atmospheres, thermogravimetric experiments were performed on blending fuels for three samples. The response surface method was used to analyze and optimize the pros and cons of different proportioning schemes to find the optimal ratio. First, the three kinds of fuels are divided into several groups according to different proportions. The different groups include one kind of fuel and a mixture of three kinds of fuel. The air atmosphere is set as 30% O_2 atmosphere, 50% O_2 atmosphere, and the heating rate of 5 K/min, 10 K/min, and 20 K/min, respectively.

3. Blended Fuel Combustion Studies

3.1. Raw Materials and Instruments. Xiaolongtan lignite (X), Yiliang tobacco rod (Y), and Fuyuan bituminous coal (F) are ground by ball mill to obtain the blended fuel with a diameter of 53~75 μm. The atmosphere in the furnace is air and O_2/CO_2 mixture containing 30% O_2, and the protective gas is high purity argon (i.e., 99.9%).

The experimental instrument is STA 449 F3 Jupiter synchronous thermal analyzer (TGDSC, Germany, NETZSCH) and corundum crucible.

3.2. Thermogravimetric Analysis. Three sample ratios were selected randomly to carry out the experiments. The results showed that the ratio of mixed coal has no influence on the pyrolysis property, while the concentration of O_2 affects this aspect. Taking the $X:Y:F$ mass ratio of 1 : 1:1 and 2 : 2 : 1 in the experiment, the thermogravimetric curves of blended coal samples under different atmospheres with a heating rate of 20 K/min are shown in Figure 1. Higher oxygen concentration in the atmosphere gives rise to a more inclined thermogravimetric curve of blended coal and increases the maximum weight loss rate, indicating that the blended coal segregates in the oxygen-rich atmosphere. With the increase of oxygen concentration, the ignition temperature and burnout temperature of the blended coal decrease dramatically, which indicates that the combustion reaction of blended coal can be completed at a lower temperature and the combustion time can be reduced, which is consistent with the results of references [14, 15].

Figure 2 shows the thermogravimetric curves of blended coal with different mass ratios at the heating rate of 20 K/min. It is noted that the curves have a similar trend. The curve is the most inclined to the high temperature zone with the $X:Y:F$ mass ratio of 0 : 2 : 1 while the curve is the most inclined to the low temperature zone with the $X:Y:F$ mass ratio of 2 : 1 : 1, indicating that the burning speed of blended coal is the fastest. Moreover, the better rate is conducive to its complete combustion [16, 17].

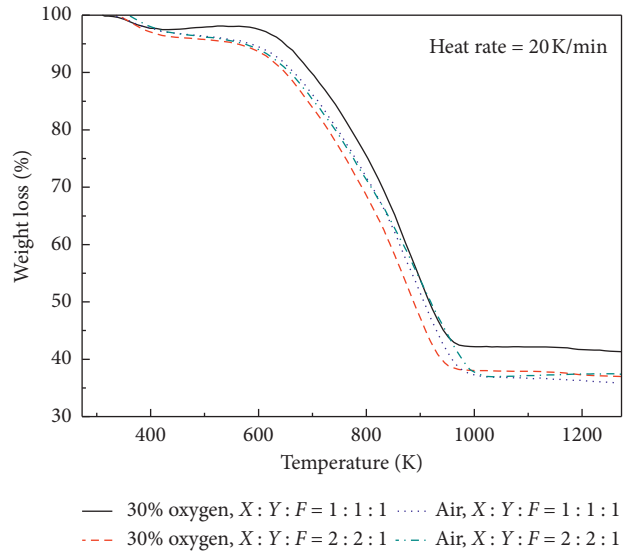

Figure 1: Effect of oxygen concentration on pyrolysis of blended coal with different mass ratios.

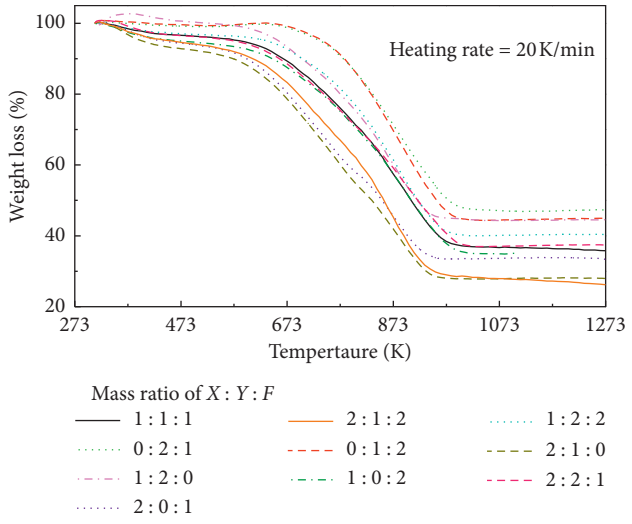

Figure 2: TG curves of mixing coals with different mass ratios.

3.3. Chemical Structure Analysis. Fuel is mainly composed of the carbon skeleton, which is surrounded by various alkyl side chains and oxygen-containing functional group branched chains. The chemical properties of the carbon skeleton are stable at low temperature, while the properties of side chains and branched chains are more active. During the combustion, the groups of side chains and branched chains are easy to participate in the chemical reactions, mainly the oxidation of active functional groups and the precipitation of volatile compounds in coal. The content of aliphatic side chains and oxygen functional groups are higher than that of lignite, which is also an essential factor leading to a better combustion performance of bituminous coal than lignite. Therefore, with the increase of the bituminous coal ratio, the combustion performance of blended fuel is gradually improved [18].

4. Decision Analysis of the Response Surface Method

4.1. Optimization of Oxygen Concentration and Heating Rate. Miscellaneous hybrid design of response surface optimization method in Design-Expert 8.0.6 software was used to design and optimize oxygen concentration and heating rate. The optimal mixing scheme was obtained by taking the combustion characteristic index and burnout temperature as the evaluation indexes. The corresponding response was filled with the calculated results based on experimental data. The design scheme and experimental evaluation indexes are shown in Table 1.

4.1.1. Combustion Characteristic Index and Variable Relation Model. Tables 2 and 3 are the variance and evaluation of the combustion characteristic indices fitted by various models, respectively. Table 4 is the confidence degree of the quadratic model. From Table 2, it is noted that the quadratic equation fits best among six models, while the cubic equation fits the worst. From Table 3, the quadratic equation has the best fitting result. Table 4 shows that the quadratic equation has a significant fitting effect and the heating rate has a significant effect on the comprehensive combustion.

Figure 3 shows the distribution of studentized residuals for the comprehensive combustion characteristic index fitting model. The dots represent comprehensive combustion characteristic indices. The red values stand for high probability while the blue values represent low probability. It is noted that the residual points are basically distributed near the straight line, indicating that the model has a good applicability. The role of the oxygen concentration and heating rate in the comprehensive combustion characteristic index is shown in Figure 4. As the oxygen concentration increases, the role of the heating rate decreases. As the heating rate increases, the role of the oxygen concentration decreases.

4.1.2. Relation Model between Burnout Temperature and Variables. Tables 5 and 6 present the variance comparisons of burnout temperatures fitted by various models. From the tables, the fitting effect of the quadratic equation is the best. Table 7 shows the confidence of the quadratic equation of the burnout temperature, which shows that the fitting effect of the quadratic model is remarkable, and the heating rate has the greatest influence on burnout temperature.

Figure 5 shows the distribution of residuals of the fitting model in Design-Expert 8.0.6. The ignition represents the burnout temperature. The red values stand for high probability while the blue values represent low probability. It is noted that the residuals are basically distributed near the straight line, which shows that the fitting effect of the model is satisfactory.

The control power of oxygen concentration and heating rate on burnout temperature is shown in Figure 6. With the increase of oxygen concentration, the control power of the heating rate increases. With the increase of heating rate, the control power of oxygen concentration increases. Therefore, in order to get the lowest burnout temperature, the heating rate and oxygen concentration can be reduced simultaneously.

Table 1: Miscellaneous design and evaluating indicator.

Sequence no.	Oxygen concentration, A (%, φ)	Heating rate, B (K/min)	Comprehensive combustion characteristic index, S ($\times 10^{-8}$)	Burnout temperature (°C)
1	50.5	20.0	20.97	516.3
2	50.5	12.5	9.26	472.9
3	80.0	12.5	13.12	419.8
4	80.0	5.0	5.91	406.2
5	50.5	5.0	3.36	422.9
6	50.5	12.5	9.81	483.7
7	80.0	20.0	39.02	427.
8	21.0	20.0	13.84	616.6
9	50.5	12.5	8.87	503.5
10	21.0	5.0	1.92	453.7
11	21.0	12.5	7.33	526.8

Table 2: The variance of comprehensive combustion characteristic index of different models.

Source of variance	Quadratic sum	Degree of freedom	Mean square	F-value	Probability > F	Scheme selection
Average value	1816.17	1	1816.17			
Linear model	763.11	2	381.56	21.27	0.0004	
2FI	100	1	100	8.12	0.0261	
Quadratic equation	83.31	2	41.66	9.48	0.0183	Recommended
Cubic equation	30.17	2	5.09	23.36	0.0041	Poor
Residual deflection	3.62	5	0.72			
Grand total	2796.38	13	215.11			

Table 3: Comprehensive evaluation of R^2 of comprehensive combustion characteristic index.

Model	Standard deviation	R^2	R^2 corrected value	R^2 predicted value	Predicted residual sum of squares	Scheme selection
Linear model	4.21	0.7984	0.7602	0.5012	541.18	
2FI	3.18	0.8617	0.8579	0.4631	606.15	
Quadratic equation	1.96	0.9366	0.9517	0.6982	327.08	Recommended
Cubic equation	0.77	0.9970	0.9914	0.6771	392.12	Poor

Table 4: The confidence of the two equations for comprehensive combustion characteristic index.

Factor	Parameter estimation	Degree of freedom	Standard deviation	95% confidence interval lower control limit	95% confidence interval upper control limit	Significant factor
Value	8.97	1.00	0.83	6.73	10.76	
Oxygen concentration, A	5.31	1.00	0.77	3.37	7.32	1.12
Heating rate, B	9.95	1.00	0.91	8.26	11.88	1.12
AB	4.83	1.00	1.02	2.26	7.27	1.12
A^2	1.47	1.00	1.03	−1.28	4.31	1.03
B^2	3.94	1.00	1.15	1.08	7.06	1.03

4.1.3. Optimizing Process Control Parameters. To make the comprehensive combustion characteristic index the largest and the burnout temperature the smallest, the experiment under certain oxygen concentration and heating rate should be optimized. The range of response index is designed in Numerical Criteria. The analysis via software results of the optimum prediction scheme is shown in Table 8. It is noted that when the oxygen concentration is 80%(φ) and the heating rate is 20 K/min, the expectation is the highest. In this case, the best results can be obtained by combining the combustion characteristic index and burnout temperature.

Figures 7 and 8 are the optimized contours and their three-dimensional response surface diagrams according to the relationship between the oxygen concentration and heating rate using the optimized scheme 1. Contours represent the specific values of the significant factors in different intervals of the target value, and their shapes reflect the interaction between the independent variables to control the effect of variables. Figure 7 shows the contours change from elliptic arc to monotonic shape with oxygen concentration when the expectation is 1. The role of heating rate increases first and then decreases when the degree of expectation is less

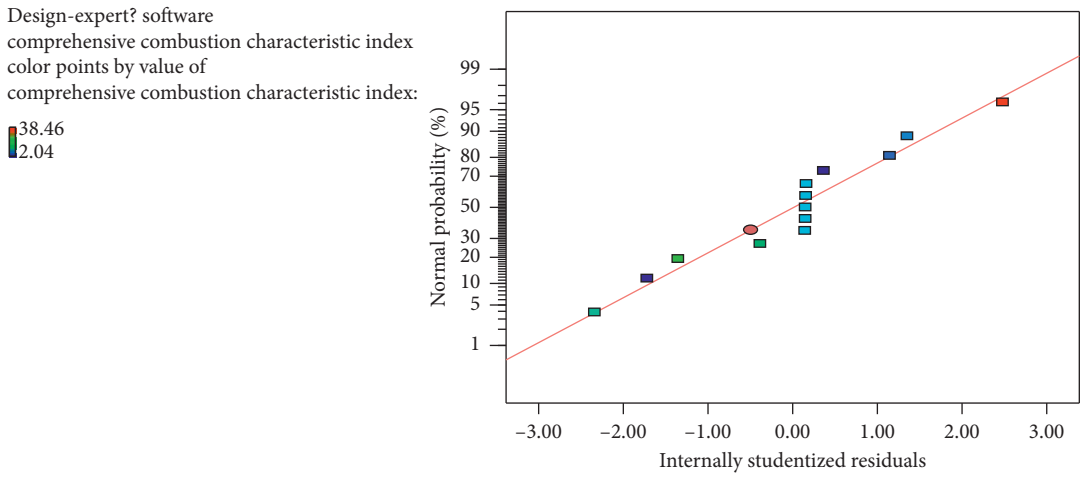

Figure 3: Distribution of the residuals of the combustible index.

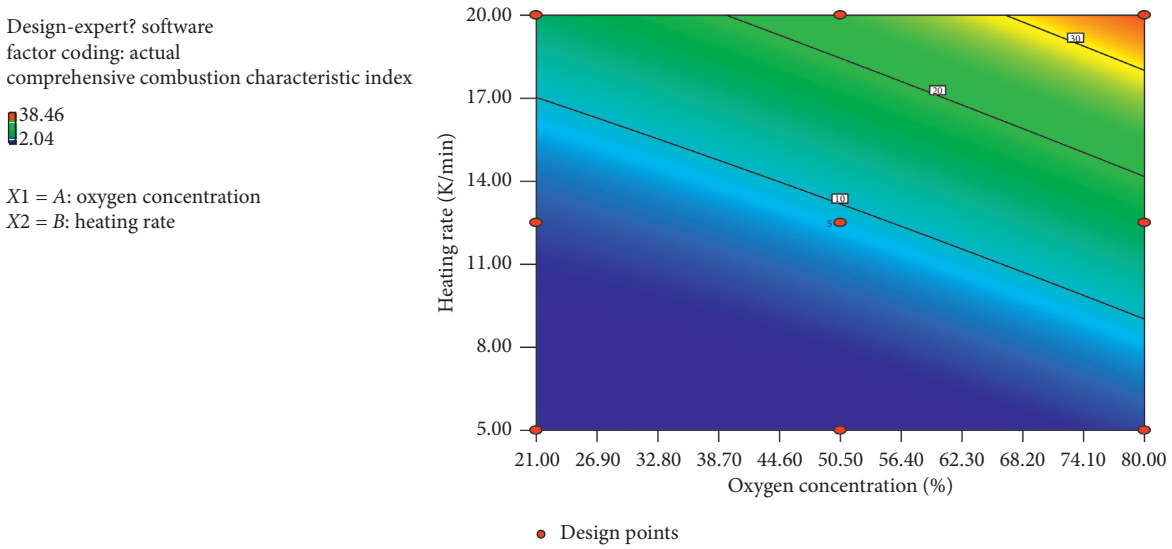

Figure 4: Response surface of comprehensive combustion characteristic index and oxygen.

Table 5: The variance of burnout temperature with different models.

Source of variance	Quadratic sum	Degree of freedom	Mean square	F-value	Probability > F	Scheme selection
Average value	3.173×10^6	1	3.173×10^6			
Linear model	33677.22	2	16838.61	32.26	<0.0001	
2FI	3987.65	1	3987.65	26.82	0.0004	
Quadratic equation	838.42	2	419.21	6.33	0.02271	Recommended
Cubic equation	128.92	2	64.46	1.08	0.37528	Poor
Residual deflection	2.96	5	0.59			
Grand total	2786.25	13	214.33			

Table 6: Comprehensive evaluation of R^2 of burnout temperature.

Model	Standard deviation	R^2	R^2 corrected value	R^2 predicted value	Predicted residual sum of squares	Scheme selection
Linear model	22.88	0.8349	0.8134	0.6525	12953.47	
2FI	11.92	0.9437	0.9391	0.9142	3388.57	
Quadratic equation	8.02	0.9817	0.9799	0.9547	3446.29	Recommended
Cubic equation	7.34	0.9917	0.9807	0.07831	34337.29	Poor

Table 7: The confidence of the two equations for burnout temperature.

Factor	Parameter estimation	Degree of freedom	Standard deviation	95% confidence interval lower control limit	95% confidence interval upper control limit	Significant factor
Value	492.77	1	3.55	483.48	502.87	
Oxygen concentration, A	−60.18	1	3.46	−64.35	−49.38	1.00
Heating rate, B	50.83	1	3.46	41.07	52.77	1.00
AB	−29.98	1	4.26	−42.66	−23.53	1.00
A^2	−13.73	1	5.18	−27.81	−2.64	1.12
B^2	−4.72	1	5.18	−15.86	6.832	1.12

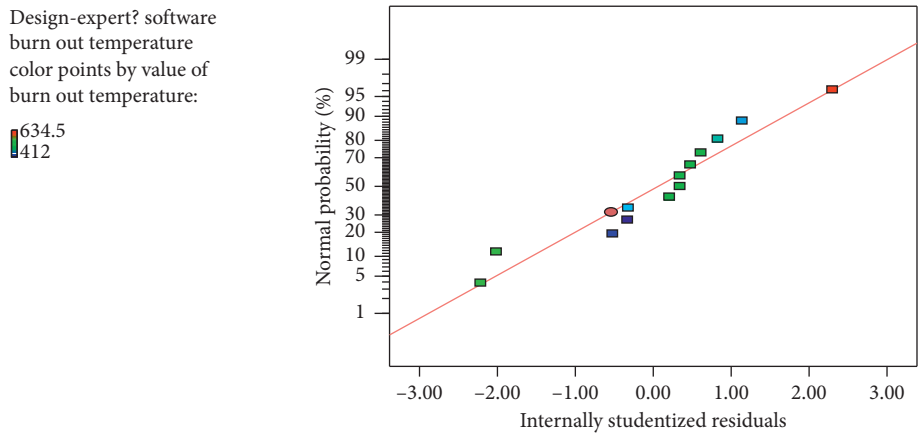

Figure 5: Distribution of the residuals of burnout temperature.

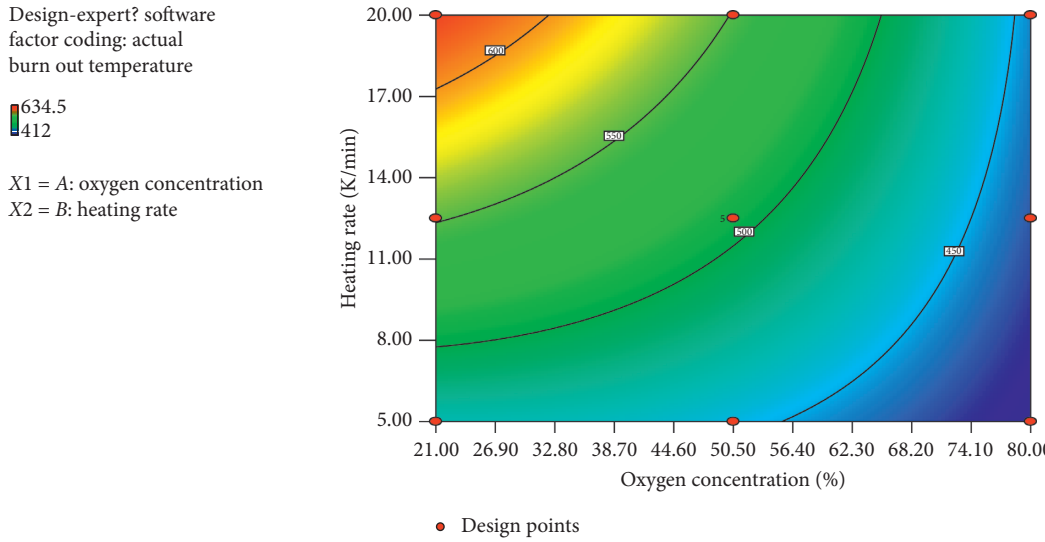

Figure 6: Response surface of the relationship between burnout temperature and oxygen concentration and heating rate.

Table 8: Comprehensive optimization scheme of various indexes of coal under different oxygen concentration and heating rate.

Sequence number	Oxygen concentration (%, φ)	Heating rate (K/min)	Comprehensive combustion characteristic index, S ($\times 10^{-8}$)	Burnout temperature (°C)	Degree of expectation
1	80.00	20.00	35.9821	438.848	0.63
2	74.82	20.00	32.6452	457.646	0.61
3	70.21	20.00	33.0137	470.325	0.53
4	21.00	5.00	3.59823	469.018	0.21

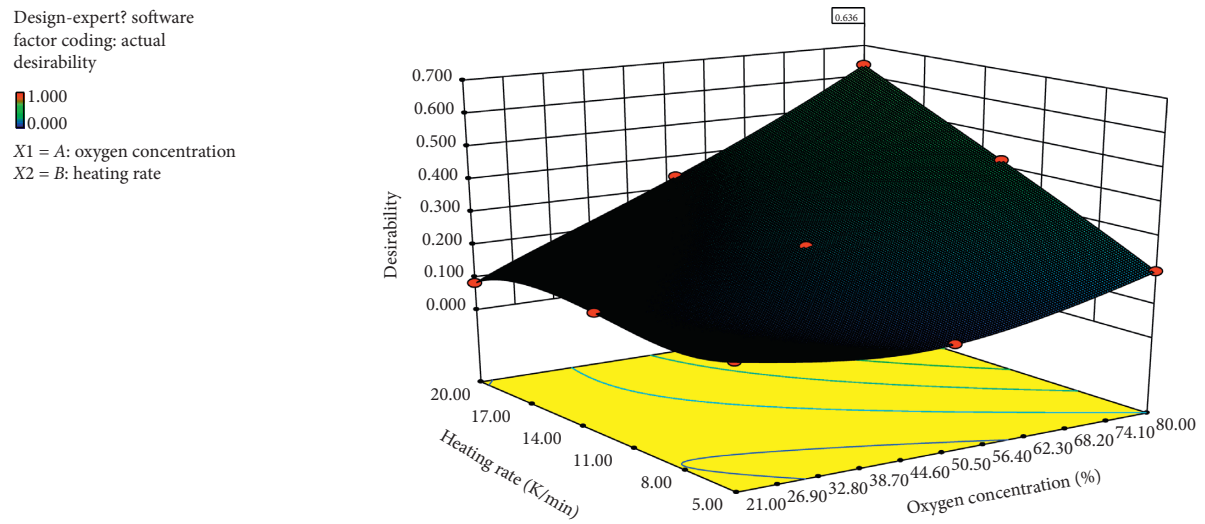

Figure 7: The optimized contour map of oxygen concentration and heating rate.

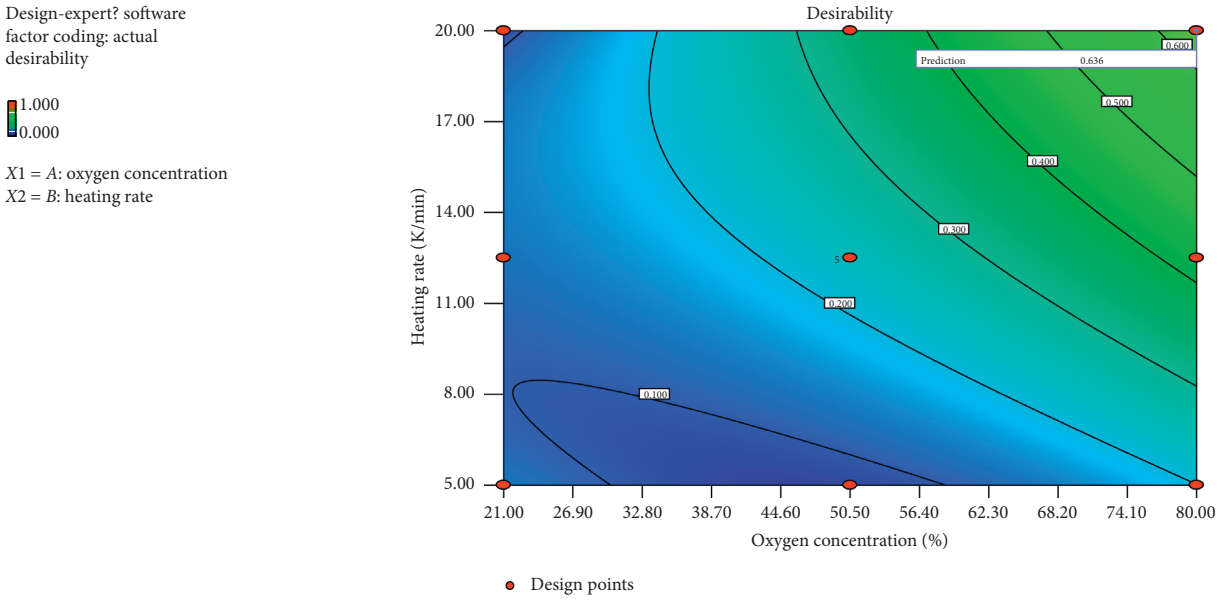

Figure 8: Expected response surface map between desirability of oxygen concentration and heating rate using optimization scheme 1.

than 1. Meanwhile, the role of heating rate increases gradually with the increase of oxygen concentration. The response surface graph of Figure 8 shows the change of expectation degree with oxygen concentration and heating rate.

4.2. Optimizing the Proportion of Blended Fuel. Design-Expert 8.0.6 software was used to design the scheme and analyze the results of the thermogravimetric experiment of blended fuel. The four evaluation indices, that is, combustibility index, comprehensive combustion characteristic index, burnout temperature, and economic cost, were optimized and the optimal mixing scheme was obtained.

For blended coal of Xiaolongtan lignite, Yiliang tobacco rod, and Fuyuan bituminous, a total of 27 groups of orthogonal experiments with 3 factors and 3 levels are needed. The Design-Expert 8.0.6 Box-Behnken is used to carry out the partial orthogonal experiments. The experimental points are the skeleton points of the experimental model according to the software and model analysis. As shown in Figure 9, there are four repetitive points on each surface of the model skeleton. The designed repetitive experimental group also needs repetition. If the same set of experimental data is used for analysis, the results of the model are inaccurate.

According to the design scheme, the corresponding response column is filled according to the calculation results of the experimental data. The designed scheme and the experimental evaluation index are shown in Table 9. It can be seen that the trend of the change of the combustibility index is generally the same as that of the comprehensive combustion characteristic index, and the combustibility index is taken for analysis.

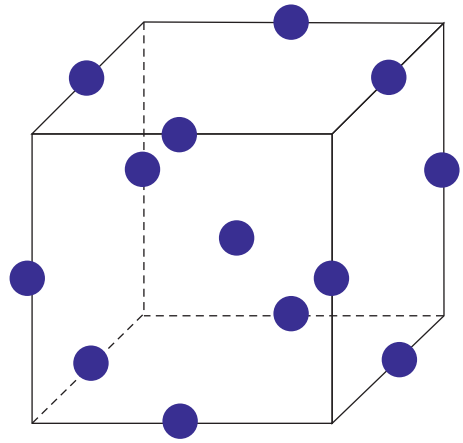

Figure 9: Test point distribution of three-factor BBD experimental design.

Table 9: Design and results of Box-Behnken orthogonal experiment.

Experiment no.	Mass ratio of $X:Y:F$	Combustible index ($\times 10^{-7}$)	Comprehensive combustion characteristic index, S ($\times 10^{-10}$)	Burnout temperature (°C)	Cost (¥/t)
1	1 : 1 : 1	35.931	3.25673	701	383
2	1 : 1 : 1	34.627	3.10528	700	383
3	1 : 1 : 1	34.153	3.26527	695	383
4	1 : 1 : 1	33.647	3.32489	701	383
5	1 : 1 : 1	35.743	3.25432	703	383
6	2 : 1 : 0	42.584	4.39395	691	296
7	1 : 2 : 2	27.709	2.48589	695	398
8	0 : 1 : 0	11.147	1.23162	707	286
9	2 : 0 : 1	30.328	2.98336	679	363
10	2 : 1 : 2	50.632	5.46327	678	402
11	1 : 0 : 0	11.475	1.18341	668	276
12	1 : 2 : 0	37.871	3.42526	676	265
13	1 : 0 : 2	33.013	3.68168	709	488
14	0 : 2 : 1	27.871	1.99386	716	378
15	2 : 2 : 1	31.987	2.68282	718	351
16	0 : 1 : 2	30.166	2.25216	709	497
17	0 : 0 : 1	4.739	0.41678	742	606

4.2.1. Relation Model between Combustibility Index and Variables. Table 10 shows the flammability index variance of blended coal of different proportions, which can be fitted by various models. From the table, the quadratic model has the best fitting effect, which is recommended for the system. The fitting effect of the cubic equation is the poorest. Table 11 compares the standard deviation, R2, and its correction value, predicted value, and squared sum of predicted residual of four fitting polynomial models. Apparently, the results show that the quadratic equation has the best fitting results.

Table 12 shows the results of software analysis on the quadratic equation and the confidence of the influencing factors. It shows that the quadratic equation fitting effect is remarkable, and the interaction between rich source bituminous coal and rich source bituminous coal has the greatest influence on the flammability index.

4.2.2. Optimizing the Proportion of Blended Fuel. Figure 10 is the distribution of the residual of the flammability index fitting model. The point represents the flammability index. The red values stand for high probability while the blue values represent low probability. It is noted that the residuals are basically distributed near the straight line, which shows that the simulation effect of the model is very good.

Figure 11 shows the relationship between the ratio of the other two samples and the flammability index when the ratio of Fuyuan bituminous coal is 50%. When the flammability index is less than 20, the control power of Yiliang tobacco rod decreases with the increase of Xiaolongtan lignite. When the flammability index is 30, the content of Xiaolongtan lignite decreases first and then increases with the increase of Yiliang smoke stem.

Table 10: The variance of combustibility index using different models.

Source of variance	Quadratic sum	Degree of freedom	Mean square	F-value	Probability > F	Scheme selection
Quadratic sum	15973.686	1	15973.686			
Linear model	1298.897	3	432.9657	6.3769	0.0059	
2FI	368.196	3	122.732	2.4367	0.1213	
Quadratic equation	356.962	3	118.9873	8.896	0.0078	Recommended
Cubic equation	96.981	3	32.327	137.234	0.0002	Poor
Residual deflection	0.924	4	0.231			
Grand total	18095.65	17	1064.45			

Table 11: Comprehensive evaluation of R^2 of combustibility index.

Model	Standard deviation	R^2	R^2 corrected value	R^2 predicted value	Predicted residual sum of squares	Scheme selection
Linear model	7.986	0.599	0.538	0.219	1706.486	
2FI	7.038	0.736	0.667	0.081	2003.612	
Quadratic equation	3.476	0.946	0.878	0.302	1613.548	Recommended
Cubic equation	0.513	1.000	0.998			Poor

Table 12: The confidence of the two equations for combustibility index.

Factor	Parameter estimation	Degree of freedom	Standard deviation	95% confidence interval lower control limit	95% confidence interval upper control limit	Significant factor
Value	3.25	1	0.55	2.26	4.58	
Xiaolongtan lignite, A	−0.51	1	0.44	−1.32	0.63	1.00
Yiliang tobacco stem, B	−1.86	1	0.44	−2.58	−0.59	1.00
Fuyuan bituminous coal, C	−2.33	1	0.44	−3.02	−1.32	1.00
AB	0.61	1	0.63	−0.87	1.79	1.00
AC	2.52	1	0.63	0.99	3.58	1.00
BC	2.31	1	0.63	0.71	3.27	1.00
A^2	0.02	1	0.60	−1.37	1.54	1.01
B^2	−0.41	1	0.60	−1.65	1.22	1.01
C^2	2.67	1	0.60	1.24	3.76	1.01

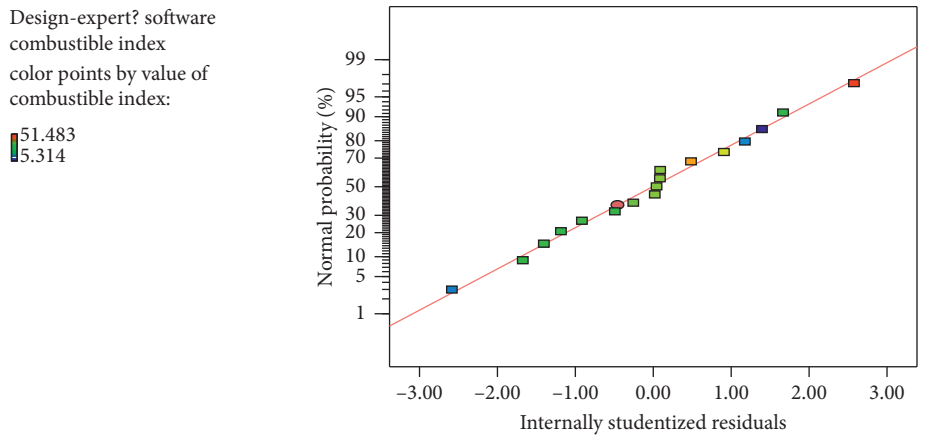

Figure 10: Distribution of the residuals of the combustible index.

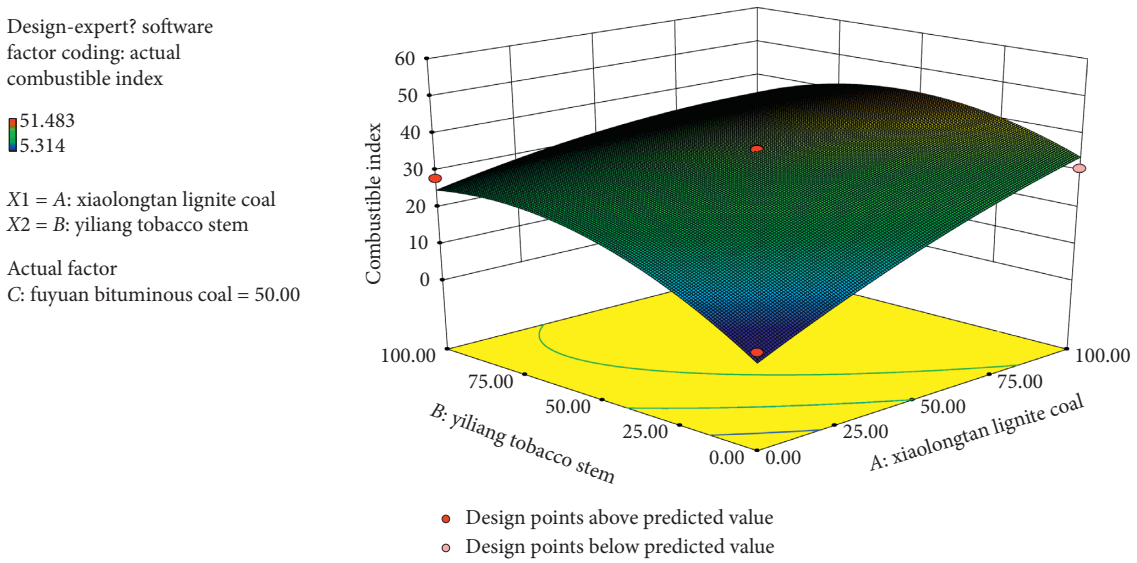

Figure 11: Response surface of the relationship between combustible index of mixing fuels and mass ratios of Xiaolongtan lignite and Yiliang tobacco rod.

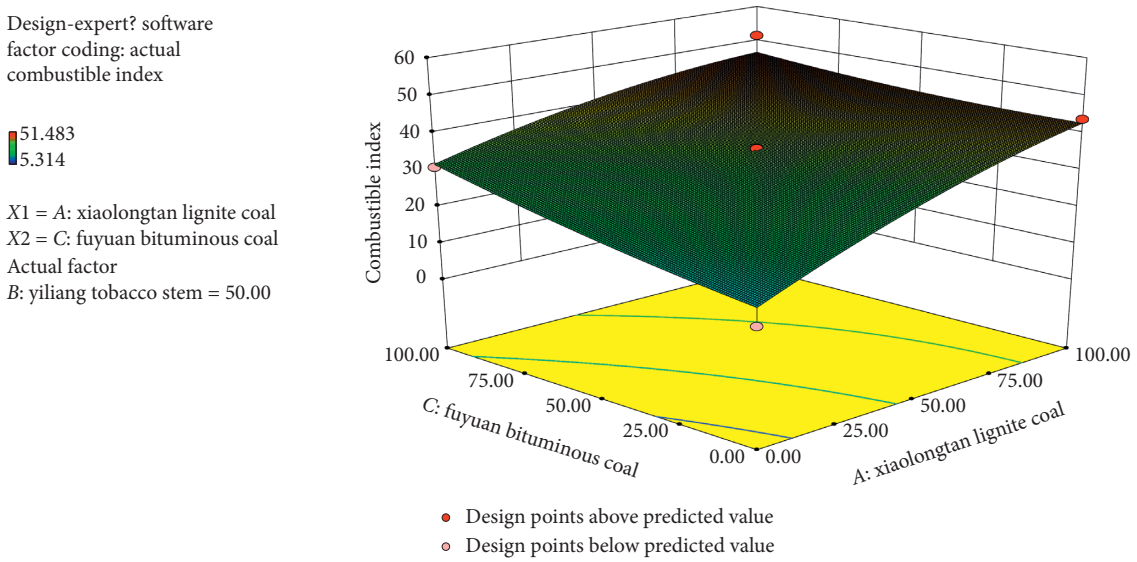

Figure 12: Response surface of the relationship between combustible index of mixing coals and mass ratios of Xiaolongtan lignite and Fuyuan bituminous coal.

Figure 12 shows the relationship between the proportion of the other two kinds of coals and the combustibility index when the proportion of Yiliang tobacco rod is 50%. The combustibility index increases with the increase of Xiaolongtan lignite and the combustibility index increases with the increase of rich source bituminous coal. Based on the fitting of experiment and model, the experiment is optimized by using Design-Expert 8.0.6 software, and the combustibility index, burnout temperature, and economic cost are optimized. In the best case, we can find the optimal mixing ratio scheme. Design Criteria of Design-Expert 8.0.6 software are also used to design the range of values of each factor and set the flammability index and combustion characteristic index to be the largest and the burnout temperature and investment cost to be the smallest.

Through the analysis, the optimal prediction scheme is shown in Table 13. From the optimization results, scheme 1 is the optimal mixing ratio, which is also suggested by the software. Xiaolongtan lignite: Yiliang tobacco rod: Fuyuan bituminous coal mass ratio is 100 : 55.12 : 1. Under this

Table 13: Comprehensive optimization scheme of each index.

Sequence no.	Mass ratio (%)			Combustible index $\times 10^{-7}$	Combustion performance index $\times 10^{-10}$	Burnout temperature (°C)	Investment cost (¥/t)	Degree of expectation
	Xiaolongtan lignite	Yiliang tobacco stem	Fuyuan bituminous coal					
1	100.00	55.12	1.00	43.3574	4.19875	678.112	251.688	0.885
2	100.00	55.64	1.00	43.4866	4.14176	678.332	251.534	0.885
3	99.58	55.12	1.00	43.3305	4.32126	678.862	251.378	0.884
4	99.37	56.37	1.00	43.4927	4.38726	678.375	250.023	0.885
5	98.22	56.81	1.00	43.3993	4.32462	678.562	251.638	0.884
6	97.62	56.13	1.00	43.2784	4.14324	679.012	251.868	0.883
7	96.88	57.66	1.00	43.2642	4.14389	679.326	250.658	0.881
8	95.79	67.86	1.00	43.9873	4.19868	685.465	241.678	0.872
9	100.00	35.87	1.32	39.9855	3.96782	670.483	266.714	0.843
10	100.00	46.02	36.83	43.0117	4.15865	692.821	322.933	0.804
11	100.00	36.33	100.00	46.9865	5.19546	682.757	438.268	0.793
12	100.00	35.05	100.00	48.0963	5.29232	682.962	439.393	0.793
13	99.27	36.78	100.00	47.6752	5.18383	682.878	439.887	0.794
14	100.00	33.89	87.279	45.8892	4.98712	690.009	420.653	0.788
15	100.00	41.02	71.43	44.5671	4.53527	692.656	386.848	0.782

condition, the model predicts that the combustibility index of blended fuel is 43.3574×10^{-7}, the combustion characteristic index is $4.27 \times 10^{-10,}$ the burnout temperature is 678.112°C, and the cost is 251.688 ¥/t, demonstrating that the expectation is the highest.

5. Conclusion

In this work, the response surface methodology was used to optimize the oxygen concentration, heating rate, and pulverized coal ratio. The effects of coal ratio on the combustibility index, combustion characteristic index, burnout temperature, and the investment cost of blended coal were analyzed. The following conclusions can be drawn:

(1) In the oxygen-enriched atmosphere, the overall precipitation of mixed coal becomes better. With the increase of oxygen concentration, the combustion rate increases, and the influence of oxygen concentration is greater than that of mixing proportion. Meanwhile, the ignition temperature and burnout temperature of pulverized coal decrease significantly, indicating that the pulverized coal can be burned at the lower temperature and combustion time can be shortened under the oxygen-enriched condition.

(2) When the expectation is 1, the role of heating rate increases first and then decreases with the increase of oxygen concentration. When the expectation is less than 1, the control force of heating rate increases gradually with the increase of oxygen concentration.

(3) Setting the flammability index and combustion characteristic index to be the largest, the burnout temperature and investment cost will be the smallest. The optimal prediction scheme 1 is the case that the mass ratio of Xiaolongtan lignite: Yiliang tobacco rod: Fuyuan bituminous coal is 100 : 55.12 : 1. Under this condition, the model predicts that the combustibility index of blended fuel is 43.3574×10^{-7}, the combustion characteristic index is 4.27×10^{-10}, the burnout temperature is 678.112°C, and the cost is 251.688 ¥/t.

Data Availability

The data used to support the findings of this study are available from the corresponding author upon request.

Conflicts of Interest

The authors declare that there are no conflicts of interest.

Acknowledgments

This work was supported by the National Natural Science Foundation of China under Grant nos. 51966005 and 51566005.

References

[1] J. Yu, L. K. Gross, and C. M. Danforth, "Complex dynamic behavior during transition in a solid combustion model," *Complexity*, vol. 14, no. 6, pp. 9–14, 2009.

[2] X. Feng, S. Huo, J. Zhang, and H. Shen, "Fuzzy predictive temperature control for a class of metallurgy lime kiln models," *Complexity*, vol. 21, no. S2, pp. 249–258, 2016.

[3] O. Kupervasser, "Laplacian growth without surface tension in filtration combustion: analytical pole solution," *Complexity*, vol. 21, no. 5, pp. 31–42, 2016.

[4] S. Su, J. H. Pohl, D. Holcombe, and J. A. Hart, "Techniques to determine ignition, flame stability and burnout of blended coals in p.f. power station boilers," *Progress in Energy and Combustion Science*, vol. 27, no. 1, pp. 75–98, 2001.

[5] D. L. Chen and L. Li, "Technical measures of HG 1025 t/h boiler burning mixed coal in shimen power plant," *Central China Electric Power*, vol. 9, no. 3, pp. 30–35, 1996.

[6] J. D. Zhang and D. L. Chen, "Characteristics of mixed coal combustion technology of 1021 t/h boiler in shimen power

plant," *Journal of Changsha Electric Power College*, vol. 11, no. 1, pp. 58–63, 1996.

[7] Z. Y. Gao, L. J. Fang, T. Wang et al., "Experimental study on kinetic parameters of blended coal combustion," *Boiler Technology*, vol. 31, no. 11, pp. 32–35, 2000.

[8] J. Haas, M. Tamura, and R. Weber, "Characterisation of coal blends for pulverised fuel combustion," *Fuel*, vol. 80, no. 9, pp. 1317–1323, 2001.

[9] A. M. Carpenter, "Coal blending for power stations," *Fuel and Energy Abstracts*, vol. 37, no. 2, pp. 84–87, 1996.

[10] B.-H. Lee, S.-I. Kim, S.-M. Kim, D.-H. Oh, S. Gupta, and C.-H. Jeon, "Ash deposition characteristics of Moolarben coal and its blends during coal combustion," *Korean Journal of Chemical Engineering*, vol. 33, no. 1, pp. 147–153, 2016.

[11] D. Peratla, N. P. Paterson, D. R. Dugwell et al., "Coal blend performance during pulverized-fuel combustion: estimate of relative relativities by a bomb-calorimeter test," *Fuel*, vol. 80, no. 11, pp. 1623–1634, 2001.

[12] J. C. V. Dyk, "Development of an alternative laboratory method to determine thermal fragmentation of coal sources during pyrolysis in the gasification process," *Fuel*, vol. 80, no. 2, pp. 245–249, 2001.

[13] X. J. Wang, *Study on the Combustion of Blended Coals*, Huazhong University of Science and Technology, Wuhan, China, 2002.

[14] Z. D. Shi, "Experimental study on several kinds of coal blending characteristics," *Power Engineering*, vol. 17, no. 2, pp. 16–20, 1997.

[15] J. R. Qiu, Y. Y. Ma, H. C. Zeng et al., "The characteristics of the mixing of coal and the degree of the coal quality and the degree of the slag," *Thermal Power Engineering*, vol. 9, no. 1, pp. 3–8, 1994.

[16] J. J. Murphy and C. R. Shaddix, "Combustion kinetics of coal chars in oxygen-enriched environments," *Combustion and Flame*, vol. 144, no. 4, pp. 710–729, 2006.

[17] P. S. Bauer, "Control coal quality through blending," *Fuels and Fuel Handling*, vol. 3, no. 3, pp. 52–55, 1981.

[18] H. Zhang, J. L. Zhang, R. S. Xu et al., "Coal and bituminous coal mixed combustion characteristics and mechanism analysis," *China Metallurgy*, vol. 26, no. 2, pp. 7–12, 2016.